7-1-2019

Bacteriophage inactivation as a function of ferrous iron oxidation

Joe Heffron
Marquette University

Brad McDermid
Marquette University

Brooke K. Mayer
Marquette University, Brooke.Mayer@marquette.edu

Environmental Science : Water Research and Technology, Vol. 5 (2019): 1309-1317. DOI.

Bacteriophage inactivation as a function of ferrous iron oxidation

Joe Heffron
Department of Civil, Construction and Environmental Engineering, Marquette University, Milwaukee, WI
Brad McDermid
Department of Civil, Construction and Environmental Engineering, Marquette University, Milwaukee, WI
Brooke K. Mayer
Department of Civil, Construction and Environmental Engineering, Marquette University, Milwaukee, WI

Abstract

Iron-based disinfection has been promoted as a potential low-cost, low-byproduct means of virus mitigation. This research is the first to establish that virus inactivation due to ferrous iron is impacted both by the extent of iron oxidation (from ferrous to ferric iron) and the rate of iron oxidation. Log inactivation of bacteriophages increased linearly with ferrous iron concentration at low doses (< 3 mg/L Fe), but higher doses limited disinfection, likely due to floc formation. The rate of iron oxidation was controlled by independently varying pH and dissolved oxygen concentration. Bacteriophage inactivation increased with the inverse of ferrous oxidation

rate, suggesting that slower iron oxidation rates allow better contact between viruses and reactive ferrous iron. Ferrous iron showed potential for disinfection in conditions of low pH and dissolved oxygen, though these conditions preclude effective iron coagulation/flocculation.

Keywords:

virus, disinfection, ferrous iron, drinking water, coagulation

1. Introduction

Waterborne viruses are a pervasive source of gastric and respiratory illnesses, both acute and chronic.[1,2] The World Health Organization's (WHO) Guidelines for Drinking Water Quality[3] identifies eight enteric viruses of concern for drinking water, all of which have high infectivity and persistence in the environment relative to other pathogens. Though enteric viruses in general are classified as “moderately tolerant” to chlorine disinfection by the U.S. Centers for Disease Control and Prevention,[4] adenoviruses are particularly resistant to UV disinfection.[5] With diameters generally less than 100 nm,[6] enteric viruses are also less susceptible to particle separation than other pathogens.[7]

Water treatment technologies featuring various iron species have attracted attention in virus mitigation research. Such technologies include iron oxide-augmented sand filtration,[8,9] iron-embedded membranes,[10] iron granules in columns or batch reactors,[11] iron nanoparticles,[12] and electrocoagulation with iron electrodes.[13] Ferrate (FeVI) salts are currently receiving attention as a green oxidant because ferrates do not contribute to chlorinated or brominated disinfection byproducts.[14] Compared to ferrate salts, ferrous salts and zero-valent iron are inexpensive and readily available. Ferric salts are often added in water treatment as a coagulant; ferric hydroxide flocs formed from oxidizing zero-valent iron or ferrous salts could serve the same function. Therefore, iron-based oxidation could be achieved in traditional water treatment facilities with a single chemical (e.g., a ferrous salt) for a combined disinfection and coagulation treatment process.

46 Several researchers[8,11–13,15] have reported irreversible virus reduction – i.e., viruses that cannot be recovered by elution – as well as damage to viral genomes and capsid proteins using iron-based technologies.[12] These reports suggest that inactivation is a significant mechanism ofvirus mitigation in addition to charge neutralization and physical 49 adsorption to iron surfaces.[8,11–13,15] Using an enzyme-linked immunosorbent assay (ELISA) to detect a decrease in antigenicity and quantitative reverse transcriptase polymerase chain reaction (qRT-PCR) to detect genomic damage, Kim et al.[12] determined that capsid damage (lower antigenicity) was a mechanism of MS2 inactivation via ferrous iron, while genomic damage was not detected.

In the presence of dissolved oxygen, ferrous iron is oxidized to ferric iron via ferryl iron (FeIV), an unstable intermediate.[16,17] Ferryl iron is a strong oxidant with an oxidation potential of 1.4 V for the Fe^{4+}/Fe^{3+} couple,[17] slightly lower than that of hypochlorite (OCl^-/Cl^-, 1.48 V).[18] The reduction of ferryl to ferric iron can further oxidize either ferrous iron or contaminants in solution, due to either direct oxidation by ferryl iron or the production of reactive oxygen species (ROS).[16,17] The evolution of ROS using iron via the Fenton process has been well documented.[19–21] Even without the addition of hydrogen peroxide, oxidation of zero-valent iron by dissolved oxygen has been shown to generate Fenton’s reagent (ferrous iron and H_2O_2), as well as ROS associated with the Fenton reaction, such as hydroxyl ($^{\bullet}OH$) and superoxide ($^{\bullet}O2^{-}$) radicals.[12,22,23] The Fenton reaction is generally considered ineffective near neutral pH.[22] Nevertheless, researchers[12,22,24] have demonstrated the oxidative effects of zero-valent and ferrous iron near neutral pH, commonly attributed to the formation of ferryl ions ($Fe^{IV}O^{2+}$).[24,25]

Despite initial confirmation that iron-based disinfection of viruses does occur, the process is poorly understood. Near neutral pH, oxidant generation arises predominantly from the oxidation of ferrous iron by dissolved oxygen.[26] Accordingly, the oxidation of ferrous iron seems to be essential to bacteriophage inactivation in iron-based treatment.[12] Disinfection of MS2 bacteriophage due to ferrous/zero-valent iron is greatest at low pH (pH 5.5 to 6),[12,27] though generation of ROS by iron oxidation has not been observed in this range.[24,26] Therefore, rapid iron oxidation may lead to shorter exposure and therefore poorer contact between the virus and reactive ferrous iron, resulting in less efficient disinfection.

74 The goal of this research was to better delineate how the extent and rate of ferrous iron oxidation impacts bacteriophage inactivation. Bacteriophages are frequently used as surrogates for human viruses in water treatment process research.[28–32] Irreversible reduction in bacteriophage concentrations was measured to determine the degree to which the ferrous iron dose, retention time, chemical quenching, and oxidation rate impacted virus inactivation. The iron oxidation rate was altered by varying pH and dissolved oxygen. The impacts of dose, pH, and dissolved oxygen on bacteriophage inactivation were used to propose an inactivation model based on iron oxidation kinetics. In addition to advancing a model relating ferrous oxidation and inactivation, the results of this study corroborate previous research by using a virus elution method to verify that bacteriophage reduction is due to inactivation rather than physical removal via coagulation/filtration.

2. Materials and Methods

2.1. Preparation of test waters

Sodium bicarbonate (2.97 mM) was added to PureLab ultrapure water (ELGA LabWater, UK) to provide alkalinity (150 mg/L as $CaCO_3$) and prevent pH from fluctuating with the addition of varying doses of ferrous chloride. The pH was adjusted using 0.5 N HCl or NaOH as required. In tests of the effect of pH on bacteriophage inactivation, the test water was adjusted to achieve pH values between 6 and 8.5; all other tests were performed at pH 7.0. To test the effect of dissolved oxygen on bacteriophage inactivation, dissolved oxygen was adjusted by degassing the solution with argon to achieve concentrations of 0.25 to 6.5 mg/L O_2. Dissolved oxygen, pH, and conductivity were measured using a Symphony benchtop multiparameter meter (VWR, Batavia, IL).

2.2. Virus propagation and quantification

Two bacteriophages were used as surrogates for human viruses: MS2 (ATCC 15597-B1) and P22 (ATCC 19585-B1). MS2 is an F-specific coliphage with a single-stranded RNA genome (Baltimore group IV), while P22 is a tailed enterobacteria phage with a double-stranded DNA genome (Baltimore group I).[31] *Escherichia coli* C-3000 (ATCC 15597) and Salmonella enterica subsp. enterica serovar Typhimurium strain LT2 (ATCC 19585) were used as the host bacteria for MS2 and P22, respectively. Bacteriophages were propagated using the double-agar layer (DAL) method and purified by two cycles of polyethylene glycol (PEG) precipitation followed by a Vertrel XF (DuPont, Wilmington, DE) purification, as described by Mayer et al.[33] Bacteriophages were quantified using the spot titer plaque assay method as described by Beck et al.[34] Samples containing bacteriophages were diluted in tenfold series, and ten 10-µL drops of each dilution were plated. Only those sets of plaque counts that did not include zero within the 95% confidence interval were considered.

Virus inactivation was determined based on infectious virus recovery by elution in beef broth.[35,36] Homogenized solutions were sampled from reactors and vortexed 10 s with an equal volume of 6% beef broth (pH 9.5) immediately prior to dilution and plating. Recoverable viruses represented the total infectious viruses present in solution, and the reduction in viruses between untreated (control) samples and treated samples (ferrous

chloride) represented inactivated viruses. Confirmation of recovery by elution is provided in Electronic Supplementary Information (ESI) 1.

2.3. Batch reactor tests

Iron-based inactivation was performed in 200-mL polypropylene batch reactors. Bacteriophages were spiked at concentrations of approximately 10^7 PFU/mL. Ferrous chloride ($FeCl_2 \bullet 4H2_O$) or ferric chloride ($FeCl_3 \bullet 6H_2O$) was diluted in ultrapure water to a concentration of 9 mM, and then added to individual reactors to achieve target concentrations ranging from 0.25 mg/L Fe to 9.7 mg/L Fe. Reactors were stirred using magnetic stir bars (16 mm length, 8 mm diameter) at 600 rpm for 30 s after addition of the iron salt to simulate rapid mixing, and then at a slower stir rate of 60 rpm for the remainder of the retention time (flocculation). Retention time ranged from 30 s to 120 min for kinetic tests and up to 48 h for tests achieving 99% iron oxidation. For tests demonstrating bacteriophage inactivation during iron oxidation (*i.e.,* before total oxidation), an excess of sodium thiosulfate (25 g/L) was added to samples taken after partial iron oxidation to prevent further oxidation during sample dilution and plating.

Total and ferrous iron concentrations were measured using Hach FerroVer Total Iron and Ferrous Iron Reagent (Hach, Loveland, CO). Absorbance was measured at 510 nm using a Genesys 20 spectrophotometer (Thermo Fisher Scientific, Waltham, MA). Ferrous iron concentrations were measured at the same time the samples were plated for virus quantification. Total iron concentrations were measured after all samples had been plated for virus quantification.

2.4. Ferrous oxidation rates

To determine the rate of ferrous oxidation with varying pH and dissolved oxygen, the change in ferrous concentration over time was measured after addition of FeCl2 (2.5 mg/L Fe) to 3 mM bicarbonate solution with pH ranging from 5.99 to 8.06 and dissolved oxygen from 0.47 to 4.77 mg/138 L. Tests of varying pH were conducted with constant dissolved oxygen (8.5 ± 0.2 mg/L O_2); tests of varying dissolved oxygen were conducted at constant pH (6.92 ± 0.07). First-order rate constants were determined under each experimental condition by fitting exponential curves to the data, as described in ESI 2.

2.5. Rate of floc formation

Floc formation over time was measured by dynamic light scattering (DLS) using a ZetaSizer Nano-ZS (Malvern Panalytical, Worcestershire, UK). Tests of flocculation with varying ferrous doses were conducted at constant pH and dissolved oxygen (pH 6.95 ± 0.10, 8.73 mg/L O2). Ferrous chloride was added to 200-mL reactors in doses ranging from 0.26 to 12.2 mg/L Fe, as in inactivation tests. Tests of flocculation with varying pH were conducted at constant ferrous dose and dissolved oxygen (2.5 mg/L Fe, 8.5 ± 0.2 mg/L DO). Low dissolved oxygen concentrations could not be accurately measured or maintained in the DLS cuvettes, so flocculation tests were not performed with sparged water.

After addition of ferrous chloride, reactors were agitated vigorously for 10 s, and 4-mL aliquots were transferred to cuvettes for particle size measurement. Floc formation was tested within the cuvettes, by measuring particle size multiple times (7 – 10) over approximately one hour. Cuvettes were gently inverted between particle size readings to simulate gentle mixing and resuspend particles for DLS analysis. In the absence of constant stirring, the primary mechanism of macroscale flocculation in the cuvettes was likely differential settling.[37] These mixing conditions were necessary in order to collect continuous data during floc formation and avoid breaking up flocs while transferring samples. Flocculation conditions in the stirred batch reactors may have differed due to velocity gradients (G). However, differential settling is a far more important factor in macroscale flocculation

than 160 fluid shear according to curvilinear models of flocculation.[38] Moreover, these tests were not intended to exactly replicate flocculation under the conditions of the batch reactors, but rather to determine the impact of ferrous dose and pH on flocculation rates.

2.6. Data analysis

Bacteriophage inactivation was correlated to parameters of percent iron oxidation, ferrous iron dose, pH, and dissolved oxygen concentration by linear regression. Linear regressions were performed in the R statistical language using the stats package.[39] A link for the R script is provided in ESI 3. Models were evaluated for residual distribution, normality, and leverage points (Cook's distance) using the $\mathrm{plot.lm}()$ function, and significance of variables was evaluated by analysis of variance with the $\mathrm{anova}()$ function.[39] Linear regression models for mean floc size as a function of time and ferrous iron dose were developed using the same methods.

3. Results and Discussion

3.1. Extent of iron oxidation

The effect of iron oxidation was initially tested by evaluating bacteriophage inactivation over time at a dose of 1 mg/L Fe. Bacteriophage inactivation increased over time and significantly correlated to the extent of iron oxidation for both MS2 (p = 6.95x10^{-10}) and P22 (p = 3.60x10^{-9}), as shown in Figure 1A and summarized in ESI 4. However, inactivation was not linearly related to the cumulative ferrous exposure (*i.e.,* the ferrous concentration integrated over time, analogous to Ct), as predicted by Chick-Watson disinfection kinetics:

$$\ln\left(\frac{N}{N_0}\right) = -\Lambda_{CW} \int_0^t C\, dt \quad (1)$$

Ferrous iron is an indirect oxidizer, in that it must itself be oxidized to a high-valent state (e.g., by dissolved oxygen) before in turn generating an intermediate oxidant, regardless of whether that oxidant is a ROS or high-valent iron species.[16,19] Therefore, ferrous iron would likely not behave as common, "primary" oxidizers (e.g., free chlorine, chloramines, ozone, etc.), in that the ambient ferrous concentration has no effect on virus inactivation. Only the ferrous iron that becomes oxidized has an ability to inactivate viruses – thus the log-linear correlation between inactivation and ferrous oxidation (Figure 1) rather than a log-linear correlation with the cumulative impact of ferrous exposure.

Based solely on this test of the kinetics of inactivation (Fig. 1A), the correlation between inactivation and extent of iron oxidation could indicate that both phenomena are related to time. For this reason, bacteriophage inactivation was also tested over a constant retention time (30 min) using doses of sodium thiosulfate from 0.5 to 4 mg/L to retard iron oxidation to varying degrees. Iron was again added as ferrous chloride (1 mg/L Fe). Bacteriophage inactivation still significantly correlated to iron oxidation using constant retention time, as shown in Figure 1B. A summary of all model parameters is given in ESI 4. Log inactivation of the bacteriophages increased with iron oxidation. Since sodium thiosulfate is a reducing agent, this test did not rule out inactivation by secondary reactions other than ferrous oxidation. However, test results showed that inhibiting oxidants in solution led to poorer inactivation, independent of contact time.

In both the variable and constant time tests, P22 inactivation occurred more rapidly and to a far greater extent than MS2, as shown in Figure 1. We are not aware of any previous disinfection study comparing these two bacteriophages, so it is unclear if P22 is more susceptible to all oxidants than MS2, or if P22 is particularly susceptible to ferrous iron. P22 (52 – 60 nm diameter) is a larger phage than MS2 (24 – 27 nm diameter),[40,41] and may therefore have a larger exposed surface area during combined coagulation/disinfection. As a tailed

bacteriophage, P22's physical structure for attachment and penetration to host bacteria is also exposed to the environment.[42] However, we did not find any evidence in the literature as to whether or not tailed bacteriophages are more susceptible to oxidative disinfection than icosahedral phages. Beyond comparing P22 and MS2 specifically, the general relationship between virion structure and susceptibility to disinfectants is a topic requiring further research.

3.2. Ferrous iron dose

To test the impact of ferrous iron concentration on bacteriophage inactivation, inactivation tests were conducted at varying doses of ferrous chloride. Whereas the tests described in Section 3.1 evaluated the kinetics of bacteriophage inactivation during the oxidation process, these tests were conducted to achieve near-total iron oxidation. The duration of the tests was based on the time required to reach 99% oxidation under the slowest oxidizing conditions (4 h). In this way, retention time was held constant in each set of experiments.

Below approximately 3 mg/L Fe, ferrous concentration had a linear positive relationship with log inactivation, as shown in Figure 2. The direct linear correlation was significant for both MS2 (p = 6.5x10^{-7}) and P22 (p = 0.000213), as shown in ESI 4. However, log inactivation did not continue to increase linearly with ferrous doses higher than 3 mg/L Fe. At this dose, floc formation was visibly more evident than at lower doses, as shown in ESI 5. When evaluated by dynamic light scattering, both the ultimate particle size and the rate of floc formation increased with ferrous doses from 0.25 to 2 mg/L Fe at pH 6.95 ± 0.10, 8.73 mg/L dissolved oxygen (summarized in ESI 4). A two-part regression of 226 particle size as a function of time and ferrous dose determined that above 3 mg/L Fe, floc formation was more rapid and independent of ferrous concentration (see ESI 4 and 5).

Previous research[35,43] has reported that virus inclusion in flocs can inhibit chlorine disinfection. The more rapid flocculation at higher ferrous concentration likely prevents contact between the enmeshed phages and oxidizing iron. The shielding of bacteriophages within flocs thus inhibits the greater disinfection expected at higher doses. Furthermore, ferrous iron bound in particles is not available to oxidize viruses. Keenan and Sedlak[26,44] confirmed that precipitation of iron species inhibits oxidant generation. Therefore, particle formation poses another engineering hurdle for design of ferrous iron disinfection systems, as disinfection and floc formation happen simultaneously.

3.3. Rate of iron oxidation

The effect of the ferrous iron oxidation rate on inactivation was evaluated by varying the concentration of hydroxide ions (pH) and dissolved oxygen. To evaluate the effect of pH and dissolved oxygen on ferrous oxidation under our experimental conditions, ferrous iron was dosed as ferrous chloride (2.5 mg/L Fe) into 3 mM sodium bicarbonate solution under conditions of varying pH (pH 5.99 to 8.06) and dissolved oxygen (0.47 to 4.77 mg/L O_2). The decrease in ferrous iron concentration was measured over time, and an empirical, first-order oxidation rate constant, k', was calculated for each experimental condition, as detailed in ESI 2. When determining the effect of pH on k', tests were conducted at a constant dissolved oxygen concentration of 8.5 ± 0.2 mg/L. Tests determining the effect of dissolved oxygen on ferrous oxidation rate were conducted at a constant pH of 6.92 ± 0.07. As shown in Figure 3, k showed a second-order correlation to the hydroxide concentration and a first-order correlation to the dissolved oxygen concentration. These correlations are consistent with Stumm and Lee's model for ferrous oxidation:[45]

$$-\frac{d[Fe(II)]}{dt} = l[Fe(II)][O_2][OH^-]^2 \quad (2)$$

While researchers have continued to refine models of ferrous oxidation kinetics,[46–49] ferrous oxidation in low ionic strength solutions conforms well to the Stumm and Lee model between approximately pH 5 and pH 8.[50] Outside this pH range, iron oxidation rates become independent of pH.[50,51]

The relationship between log inactivation and iron oxidation rate was determined by altering either pH or dissolved oxygen concentration. Ferrous oxidation rate constants were predicted for each experimental condition using the relationships to hydroxide and dissolved oxygen concentration shown in Figure 3. Log inactivation was then modeled as a function of the ferrous oxidation rate constant. As in Section 3.2, experiments were conducted until 99% oxidation was achieved under the most limiting conditions. This time varied based on the conditions of each set of experiments: 4 h for dissolved oxygen tests and 48 h for pH tests.

3.3.1. Effect of pH on virus inactivation

Given the correlation between virus inactivation and iron oxidation, the role of pH in virus inactivation is somewhat counterintuitive. At higher pH, iron oxidation is increasingly rapid, yet bacteriophage inactivation is greater at low pH, as shown in Figure 4. Models for both MS2 and P22 showed a very strong correlation between log inactivation and the inverse of the rate constant, as predicted by pH (p values =1.92 and 2.38 x10^{-8}, respectively). Previous work by Kim et al.[12] also showed increasing log MS2 reduction at low pH with ferrous iron. Our study provides important confirmation of the MS2 inactivation observed in this earlier work, because Kim et al. did not use an elution method to ensure that bacteriophage mitigation was due to inactivation rather than virus aggregation due to charge neutralization. Kim et al. did verify inactivation qualitatively via enzyme-linked immunosorbent assay (ELISA) and qPCR. The results of our study corroborated Kim et al.'s results, and actually found a more dramatic inverse relationship between log inactivation and hydroxide concentration (Figure 4). This minor difference in results is likely due to a fundamental difference in experimental design. Since Kim's study focused on kinetics rather than carrying iron oxidation out to an endpoint, slower iron oxidation rates at low pH would lead to lower effective doses of oxidized iron. In our study, a consistent extent of iron oxidation was used, so inactivation at lower pH was not kinetically limited.

At higher pH, particles formed far more rapidly than at low pH, as shown in ESI 6. Oxidation of iron encourages precipitation of ferrous iron as mixed-valent precipitates such as magnetite.[52] In an equilibrium model of iron speciation using MINEQL+, solid magnetite ($Fe^{II}Fe^{III}_2O_{4\,(s)}$) completely replaced ferrous ions ($Fe^{2+}_{(aq)}$) as the dominant species as the stoichiometric ratio of Fe^{III} to Fe^{II} increased from 0 to 2 (ESI 6). The thermodynamic favorability of solid magnetite over ferrous ions suggests that the oxidation of ferrous iron has a negative feedback effect on further oxidation by precipitating mixed-valent particles. Though thermodynamic equilibrium models cannot predict the kinetics of speciation, magnetite is a common mixed-valent product of iron electrocoagulation and can form within seconds.[52] Therefore, competition between ferrous oxidation and co-precipitation with ferric iron is likely. Thus, faster rates of ferrous oxidation also lead to more rapid particle formation, and thereby poorer oxidant generation/availability, as discussed in Section 3.2.

Several researchers [22,26,53] have hypothesized that the intermediate oxidant evolved during iron oxidation shifts from hydroxyl radicals at low pH to a putative ferryl oxidant near neutral pH. However, hydroxyl radical generation due to iron oxidation is only relevant at pH 5 and below,[22,23,26] so no change in oxidant is anticipated in the circumneutral pH range in this study. In addition, the Fenton reaction has been shown to oxidize organic substrates to form organic radicals.[54] If ferrous iron is sorbed to the capsid surface, the formation of organic radicals may suggest an entirely different mechanism of inactivation. Further research is required to determine which intermediate oxidants are responsible for virus inactivation.

3.3.2. Effect of dissolved oxygen on virus inactivation

To confirm that a slower oxidation rate increases bacteriophage inactivation, ferrous iron disinfection was performed under a range of dissolved oxygen conditions. As shown in Figure 5, greater inactivation was observed at lower dissolved oxygen concentrations below approximately 3 mg/L, whereas inactivation was insensitive to oxygen concentration above 3 mg/L. This seeming paradox of lower dissolved oxygen resulting in greater inactivation requires special attention. Though a total lack of oxygen will inhibit ferrous oxidation, low (non-zero) concentrations of dissolved oxygen only limit ferrous oxidation kinetically. In order to isolate the impact of the rate of ferrous oxidation in this study, it was important to ensure the same extent of iron oxidation. The extent of iron oxidation was controlled by allowing sufficient time for near-total iron oxidation in all conditions. Therefore, iron oxidation was not limited under conditions of low oxygen.

For this reason, earlier work by Kim et al.[12] found overall greater MS2 inactivation by ferrous iron in air-saturated water versus deaerated water (dissolved oxygen concentration below detection), while extended reactions in our study resulted in greater inactivation at low (but measurable) dissolved oxygen. As with pH, the difference between our results and those of Kim et al. is a result of different experimental design addressing a fundamentally different objective. Kim et al. evaluated bacteriophage inactivation kinetics over the span of 1 h, rather than allowing near-total iron oxidation as in our study. Since ferrous oxidation becomes exponentially slower approaching 0 mg/L dissolved oxygen, stopping the reaction at 1 h would result in a far greater extent of iron oxidation in the aerated samples compared to the deaerated samples. In Kim et al.'s experiment, there was no difference between air-saturated and deaerated water at ferrous doses 0.1 mM and lower, the range investigated in this study, indicating that even oxygen levels below detection were sufficient to oxidize low concentrations of iron at circumneutral pH.

The regression models of the dissolved oxygen tests revealed very significant correlations between log inactivation and the inverse of the predicted ferrous oxidation rate constants for both MS2 ($p = 5.04\text{x}10^{-4}$) and P22 ($p = 2.00\text{x}10^{-4}$), as shown in ESI 4. This confirms the effect of dissolved oxygen on inactivation to a high degree of confidence. However, the dissolved oxygen models for MS2 and P22 described less of the variation in the data compared to models for other parameters in this study. The greater unexplained variation was likely due to difficulty in maintaining constant dissolved oxygen concentrations throughout the 4-hour test duration. The argon sparging process also caused a change in pH, requiring pH correction of individual reactors at very low (< 1 mg/L) dissolved oxygen concentrations. Since small changes in pH can affect inactivation (see Figure 4), pH most likely contributed to variation as well. Regression models accounting for final pH and dissolved oxygen concentrations had slightly better explanatory power ($R^2_{adj} = 0.788$ for MS2 and 0.520 for P22). Regardless, the inverse relationship to ferrous oxidation rate remained significant in the adjusted models for both bacteriophages.

3.4. Proposed model for bacteriophage inactivation via iron oxidation

As shown in Figures 4 and 5, the transition from a highly concentration-dependent inactivation to condition-independent (low) inactivation occurred at approximately pH 7.25 and 2 mg/L dissolved oxygen. Regardless of which parameter was varied, this transition corresponded to a rate constant of approximately 0.04 – 0.1 min-1. Therefore, the dependence of bacteriophage inactivation on pH and dissolved oxygen can be powerfully described using ferrous oxidation rate as the only predictor. The intermediate oxidants (whether ROS or ferryl species) are short-lived, with half-lives ranging from nanoseconds to seconds.[55,56] In addition, the reduction of ferryl iron to ferric iron can oxidize an equivalent of ferrous iron.[16,19] In this way, ferrous iron may itself compete with viruses for oxidants. Therefore, close proximity between ferrous iron and the virus may be necessary to ensure that virus inactivation can compete with ferrous autoxidation. Both MS2 and P22 are negatively charged near neutral pH,[10,57] and would therefore attract positively-charged ferrous species. A slower rate of oxidation

would allow more time for contact between virions and ferrous ions prior to inclusion of both species in flocs. Based on these results and those in Sections 3.1 and 3.2 relating bacteriophage inactivation to the extent of ferrous iron oxidation, the following relationship describes bacteriophage inactivation under the conditions of this study (i.e., ferrous dose < 3 mg/L Fe, circumneutral pH, dissolved oxygen > 0 mg/L).

$$ln\left(\frac{N}{N_0}\right) \propto -\frac{\Delta C_{Fe(II)}}{k'} \propto -\frac{\Delta C_{Fe(II)}}{[O_2][OH^-]^2} \quad (3)$$

This model predicts that greater bacteriophage inactivation can be achieved by either a greater extent of ferrous oxidation or a slower rate of ferrous oxidation. This relationship is analogous to Chick-Watson disinfection kinetics (Eqn. 1), in which cumulative exposure to a slowly degrading oxidant achieves greater inactivation than a quickly degrading oxidant. However, log bacteriophage inactivation was not linearly related to cumulative ferrous exposure (see Section 3.1), but was rather likely inhibited by competition and/or shielding of viruses from oxidation due to iron precipitation. This relationship presents an unavoidable paradox for ferrous iron in drinking water treatment, because achieving a high extent of iron oxidation is limited by the slow rate at which the oxidation must take place. High doses of iron are also self-limiting due to more rapid floc formation. Moreover, one promise of ferrous iron for drinking water treatment has been combined disinfection and coagulation/flocculation. However, the results of this study suggest that these goals, if not mutually exclusive, would require finely-tuned control of oxidation conditions to maximize disinfection before allowing flocculation to occur.

4. Conclusions

This research demonstrated that bacteriophage inactivation at circumneutral pH relies not only on the extent, but also the rate, of iron oxidation. Decreases in pH and dissolved oxygen both led to greater inactivation, therefore supporting the hypothesis that slower oxidation promotes inactivation. Though inactivation was not correlated to cumulative exposure to ferrous iron, available reactive ferrous iron was necessary for virus inactivation. Based on the hypothesized short-lived oxidants generated by iron oxidation, close contact, or even sorption of ferrous iron, to virus capsids may be necessary for inactivation. In addition, particle formation in faster ferrous oxidation conditions likely inhibited inactivation by shielding viruses and/or inhibiting oxidant generation. This research used synthetic waters to minimize variables influencing iron speciation and bacteriophage fate. However, further research must evaluate inactivation of multiple pathogens, including human viruses, in natural water conditions before ferrous oxidation can be considered relevant for drinking water.

If all ferrous iron is eventually oxidized, the slower oxidation rate achieves greater inactivation. However, for a working treatment process, whether or not all ferrous iron is oxidized is an important question. Iron oxidation may be too rapid to offer a practical means of disinfection in waters above neutral pH or saturated with dissolved oxygen, while iron oxidation may be impractically slow in groundwater or mildly acidic waters (< pH 6). Pairing iron oxidation with pH control, as in enhanced coagulation, may allow greater disinfection by retarding ferrous oxidation. However, the pH must then be increased after disinfection for the flocculation stage to encourage particle formation.

References

1 N. R. Blacklow and H. B. Greenberg, Viral gastroenteritis, *N. Engl. J. Med.*, 1991, 325, 252–264.

2 T.-T. Fong and E. K. Lipp, Enteric viruses of humans and animals in aquatic environments: Health risks, detection, and potential water quality assessment tools, *Microbiol. Mol. Biol. Rev.*, 2005, 69, 357–371.

3 World Health Organization, Ed., WHO guidelines for drinking-water quality., World Health Organization, Geneva, 4th edn., 2011.
4 Centers for Disease Control and Prevention, Effect of chlorination on inactivating selected pathogens, http://www.cdc.gov/safewater/effectiveness-on-pathogens.html, (accessed 1 January 2015).
5 C. P. Gerba, D. M. Gramos and N. Nwachuku, Comparative inactivation of enteroviruses and adenovirus 2 by UV light, *Appl. Environ. Microbiol*., 2002, 68, 5167.
6 M. Abbaszadegan, M. Lechevallier and C. P. Gerba, Occurrence of Viruses in US Groundwaters, *J. Am. Water Works Assoc.,* 2003, 95, 107–120.
7 C. T. Tanneru and S. Chellam, Sweep flocculation and adsorption of viruses on aluminum flocs during electrochemical treatment prior to surface water microfiltration, *Environ. Sci. Technol*., 2013, 47, 4612–4618.
8 J. N. Ryan, R. W. Harvey, D. Metge, M. Elimelech, T. Navigato and A. P. Pieper, Field and laboratory investigations of inactivation of viruses (PRD1 and MS2) attached to iron oxide-coated quartz sand, *Environ. Sci. Technol*., 2002, 36, 2403–2413.
9 I. Bradley, A. Straub, P. Maraccini, S. Markazi and T. H. Nguyen, Iron oxide amended biosand filters for virus removal, *Water Res*., 2011, 45, 4501–4510.
10 M. M. Fidalgo De Cortalezzi, M. V. Gallardo, F. Yrazu, G. J. Gentile, O. Opezzo, R. Pizarro, H. R. Poma and V. B. Rajal, Virus removal by iron oxide ceramic membranes, *J. Environ. Chem. Eng*., 2014, 2, 1831–1840.
11 Y. You, J. Han, P. C. Chiu and Y. Jin, Removal and inactivation of waterborne viruses using zerovalent iron, *Environ. Sci. Technol*., 2005, 39, 9263–9269.
12 J. Y. Kim, C. Lee, D. C. Love, D. L. Sedlak, J. Yoon and K. L. Nelson, Inactivation of MS2 coliphage by ferrous ion and zero-valent iron nanoparticles, *Environ. Sci. Technol*., 2011, 45, 6978–6984.
13 C. T. Tanneru and S. Chellam, Mechanisms of virus control during iron electrocoagulation--microfiltration of surface water., *Water Res*., 2012, 46, 2111–20.
14 V. K. Sharma, Oxidation of inorganic contaminants by ferrates (VI, V, and IV)-kinetics and mechanisms: A review, *J. Environ. Manage*., 2011, 92, 1051–1073.
15 T. Kohn, Lausanne, 2009.
16 L. Li, C. M. van Genuchten, S. E. A. Addy, J. Yao, N. Gao and A. J. Gadgil, Modeling As(III) oxidation and removal with iron electrocoagulation in groundwater., *Environ. Sci. Technol*., 2012, 46, 12038–45.
17 S. H. Bossmann, E. Oliveros, S. Göb, S. Siegwart, E. P. Dahlen, L. Payawan, M. Straub, M. Wörner and A. M. Braun, New evidence against hydroxyl radicals as reactive intermediates in the thermal and photochemically enhanced fenton reactions, *J. Phys. Chem. A,* 1998, 102, 5542–5550.
18 G. Sharma, J. Choi, H. K. Shon and S. Phuntsho, Solar-powered electrocoagulation system for water and wastewater treatment, *Desalin. Water Treat*., 2011, 32, 381–388.
19 H. Bataineh, O. Pestovsky and A. Bakac, pH-induced mechanistic changeover from hydroxyl radicals to iron(iv) in the Fenton reaction, *Chem. Sci*., 2012, 3, 1594–1599.
20 E. Neyens and J. Baeyens, A review of classic Fenton's peroxidation as an advanced oxidation technique, *J. Hazard. Mater*., 2003, 98, 33–50.
21 J. Pignatello, E. Oliveros and A. MacKay, Advanced oxidation processes for organic contaminant destruction based on the Fenton reaction and related chemistry, Crit. Rev. Environ. Sci. Technol., 2006, 36, 1–84.
22 I. A. Katsoyiannis, T. Ruettimann and S. J. Hug, pH dependence of Fenton reagent generation and As(III) oxidation and removal by corrosion of zero valent iron in aerated water, *Env. Sci Technol*., 2008, 42, 7424–7430.
23 T. Harada, T. Yatagai and Y. Kawase, Hydroxyl radical generation linked with iron dissolution and dissolved oxygen consumption in zero-valent iron wastewater treatment process, *Chem. Eng. J.,* 2016, 303, 611–620.

24 L. A. Reinke, J. M. Rau and P. B. Mccay, Characteristics of an Oxidant formed during Iron(II) Autoxidation, *Free Radic. Biol. Med.,* 1994, 16, 485–492.
25 J. D. Rush, Z. Maskos and W. H. Koppenol, Distinction between hydroxyl radical and ferryl species, *Methods Enzymol*., 1990, 186, 148–156.
26 C. R. Keenan and D. L. Sedlak, Factors Affecting the Yield of Oxidants from the Reaction of Nanoparticulate Zero-Valent Iron and Oxygen Factors Affecting the Yield of Oxidants from the Reaction of Nanoparticulate Zero-Valent Iron and Oxygen, *Env. Sci Technol*., 2008, 42, 1262–1267.
27 J. Y. Kim, C. Lee, D. L. Sedlak, J. Yoon and K. L. Nelson, Inactivation of MS2 coliphage by Fenton's reagent, *Water Res*., 2010, 44, 2647–2653.
28 N. Boudaud, C. Machinal, F. David, A. Fréval-Le Bourdonnec, J. Jossent, F. Bakanga, C. Arnal, M. P. Jaffrezic, S. Oberti and C. Gantzer, Removal of MS2, Qβ and GA bacteriophages during drinking water treatment at pilot scale, *Water Res*., 2012, 46, 2651–2664.
29 O. Ferrer, R. Casas, C. Galvañ, F. Lucena, A. Vega, O. Gibert, J. Jofre and X. Bernat, Challenge tests with virus surrogates: an accurate membrane integrity evaluation system?, *Desalin. Water Treat*., 2013, 51, 4947–4957.
30 M. Amarasiri, M. Kitajima, T. H. Nguyen, S. Okabe and D. Sano, Bacteriophage removal efficiency as a validation and operational monitoring tool for virus reduction in wastewater reclamation: *Review, Water Res*., 2017, 121, 258–269.
31 W. O. K. Grabow, Bacteriophages: Update on application as models for viruses in water, *Water SA*, 2001, 27, 251–268.
32 J. Heffron and B. K. Mayer, Virus mitigation by coagulation: recent discoveries and future directions, *Environ. Sci. Water Res. Technol.,* 2016, 2, 443–459.
33 B. K. Mayer, H. Ryu and M. Abbaszadegan, Treatability of U.S. Environmental Protection Agency contaminant candidate list viruses: Removal of coxsackievirus and echovirus using enhanced coagulation, *Environ. Sci. Technol.,* 2008, 42, 6890–6896.
34 N. K. Beck, K. Callahan, S. P. Nappier, H. Kim, M. D. Sobsey and J. S. Meschke, Development of a spot-titer culture assay for quantifying bacteria and viral indicators, *J. Rapid Methods Autom. Microbiol*., 2009, 17, 455–464.
35 C. T. Tanneru, N. Jothikumar, V. R. Hill and S. Chellam, Relative insignificance of virus inactivation during aluminum electrocoagulation of saline waters., *Environ. Sci. Technol*., 2014, 48, 14590–8.
36 B. Zhu, D. A. Clifford and S. Chellam, Virus removal by iron coagulation-microfiltration., *Water Res*., 2005, 39, 5153–5161.
37 J. C. Crittenden, R. R. Trussell, D. W. Hand, K. J. Howe and G. Tchobanoglous, *MWH's Water Treatment: Principles and Design*, John Wiley & Sons, Inc., Hoboken, New Jersey, 3rd edn., 2012.
38 M. Han and D. F. Lawler, The (relative) insignificance of G in flocculation, *J. Am. Water Works Assoc*., 1992, 84, 79–91.
39 R Core Team, 2014.
40 C. Shen, M. S. Phanikumar, T.-T. Fong, I. Aslam, S. P. Mcelmurry, S. L. Molloy and J. B. Rose, Evaluating bacteriophage P22 as a tracer in a complex surface water system: The Grand River, Michigan, *Environ. Sci. Technol.,* 2008, 42, 2426–2431.
41 B. K. Mayer, Y. Yang, D. W. Gerrity and M. Abbaszadegan, The impact of capsid proteins on virus removal and inactivation during water treatment processes, *Microbiol. Insights*, 2015, 8, 15–28.
42 P. E. Prevelige, in *The Bacteriophages*, ed. R. Calendar, 1988, pp. 457–468.
43 S. Ohgaki and P. Mongkonsiri, in *Chemical Water and Wastewater Treatment*, eds. H. H. Hahn and R. Klute, Springer Verlag, Heidelberg, 1990, pp. 75–84.
44 C. R. Keenan and D. L. Sedlak, Ligand-enhanced reactive oxidant generation by nanoparticulate zero-valent iron and oxygen, *Env. Sci Technol*., 2008, 42, 6936–6941.

45 W. Stumm and F. G. Lee, Oxygenation of ferrous iron, *Ind. Eng. Chem*., 1961, 53, 143–146.
46 D. W. King, Role of carbonate speciation on the oxidation rate of Fe(II) in aquatic systems, *Environ. Sci. Technol*., 1998, 32, 2997–3003.
47 F. J. Millero, S. Sotolongo and M. Izaguirre, Oxidation kinetics of Fe (II) in sea water, *Geochim. Cosmochim. Acta*, 1987, 51, 793–801.
48 B. A. Dempsey, H. C. Roscoe, R. Ames, R. Hedin and B.-H. Jeon, Ferrous oxidation chemistry in passive abiotic systems for the treatment of mine drainage, *Geochemistry Explor. Environ. Anal*., 2011, 1, 81–88.
49 J. M. Santana-Casiano, M. González-Dávila and F. J. Millero, The role of Fe(II) species on the oxidation of Fe(II) in natural waters in the presence of O2 and H2O2, *Mar. Chem*., 2006, 99, 70–82.
50 B. Morgan and O. Lahav, The effect of pH on the kinetics of spontaneous Fe(II) oxidation by O2 in aqueous solution - basic principles and a simple heuristic description, *Chemosphere*, 2007, 68, 2080–2084.
51 P. C. Singer and W. Stumm, Acidic Mine Drainage: The Rate-Determining Step, *Science* (80-.)., 1970, 167, 1121–1123.
52 K. L. Dubrawski, C. M. Van Genuchten, C. Delaire, S. E. Amrose, A. J. Gadgil and M. Mohseni, Production and transformation of mixed-valent nanoparticles generated by Fe(0) electrocoagulation, *Environ. Sci. Technol.,* 2015, 49, 2171–2179.
53 S. J. Hug and O. X. Leupin, Iron-catalyzed oxidation of arsenic (III) by oxygen and by hydrogen peroxide: pH-dependent formation of oxidants in the Fenton reaction RN - Environ. Sci. Technol., vol. 37, pp. 2734-2742, 2003, 37, 2734–2742.
54 S. Goldstein, D. Meyerstein and G. Czapski, The Fenton reagents, *Free Radic. Biol. Med*., 1993, 15, 435–445.
55 J. He, X. Yang, B. Men and D. Wang, Interfacial mechanisms of heterogeneous Fenton reactions catalyzed by iron-based materials: A review, *J. Environ. Sci. (China),* 2016, 39, 97–109.
56 Oleg Pestovsky and A. Bakac, in *Ferrates*, 2008, pp. 167–176.
57 B. K. Mayer, Y. Yang, D. W. Gerrity and M. Abbaszadegan, The impact of capsid proteins on virus removal and inactivation during water treatment processes, *Rev*.

Figures

A) Varying time

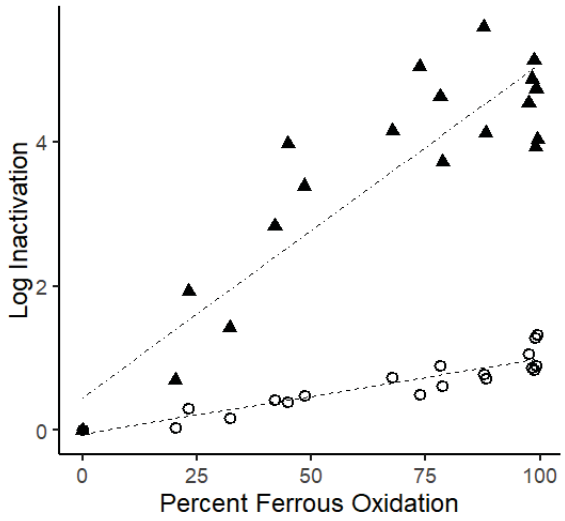

B) Varying sodium thiosulfate dose

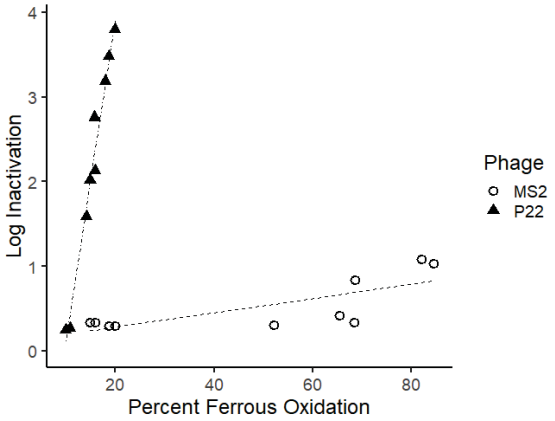

Figure 1. Increasing bacteriophage inactivation with ferrous iron oxidation. Iron oxidation was controlled by varying A) time (0.5 to 120 min), and B) sodium thiosulfate dose (0.5 to 4 mg/L). Iron was added as ferrous chloride (1 mg/L Fe). Over a constant retention time of 30 min, bacteriophage inactivation correlated with iron oxidation. Each point represents a single experiment.

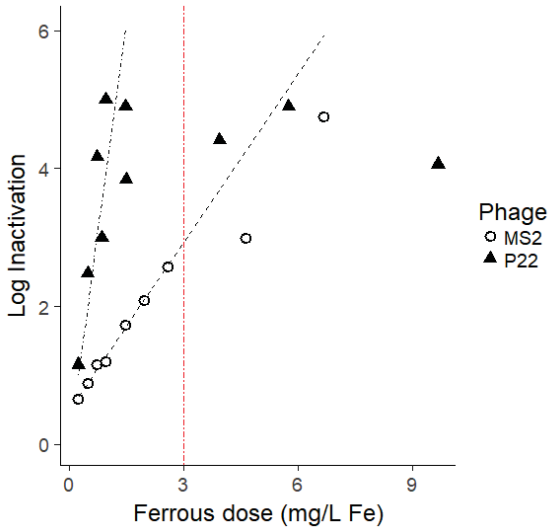

Figure 2. The effect of ferrous iron dose on bacteriophage inactivation. Below approximately 3 mg/L Fe (indicated by the vertical red line), both phages showed an approximately linear relationship between ferrous iron concentration and log inactivation, as illustrated by the regression trendlines. Log inactivation did not linearly increase with higher ferrous doses. Each point represents a single experiment.

(A) Hydroxide concentration / pH

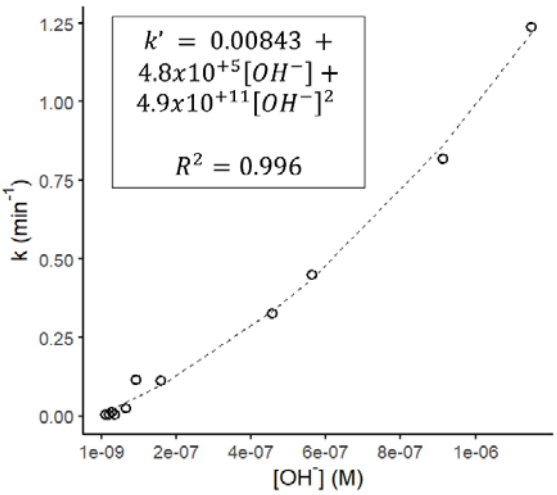

(B) Dissolved oxygen concentration

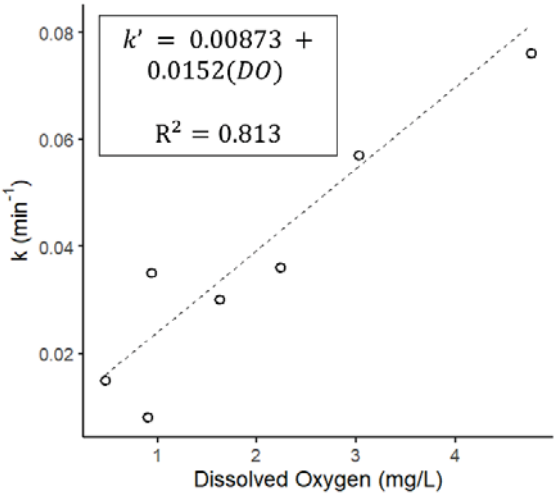

Figure 3. 552 First-order ferrous oxidation rate constants as a function of (A) pH/hydroxide concentration and (B) dissolved oxygen. The second-order correlation to hydroxide concentration and first-order correlation to dissolved oxygen concentration are in accordance with established kinetic models for ferrous oxidation.

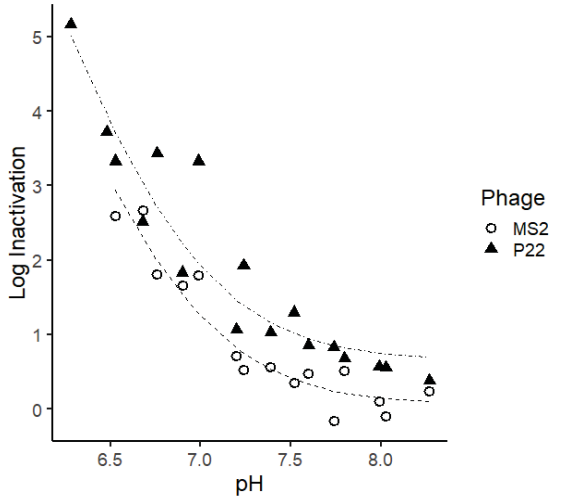

Figure 4. Effect of pH o 559 n bacteriophage reduction by ferrous iron (0.5 mg/L Fe). Both phages showed an approximately inverse relationship between greater ferrous oxidation rate (achieved here by increasing pH/hydroxide concentration) and bacteriophage inactivation, as illustrated by the regression trendlines. Each point represents a single experiment.

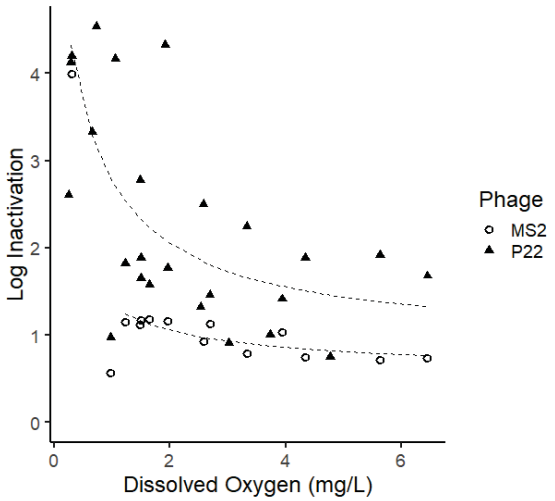

Figure 5. Effect of dissolved oxygen on bacteriophage inactivation by iron oxidation (0.5 mg/L Fe). Both phages showed an approximately inverse relationship between greater ferrous oxidation rate (achieved here by increasing dissolved oxygen concentration) and bacteriophage inactivation, as illustrated by the regression trendlines. Each point represents a single experiment.